Magnetic properties of Mn-Zn ferrites under DC bias conditions

Čedo Žlebič
Univerzitet u Novom Sadu Fakultet tehnickih nauka
Miodrag Milutinov (miodragm@uns.ac.rs)
Univerzitet u Novom Sadu https://orcid.org/0000-0002-1725-3405
Maria Vesna Nikolić
Univerzitet u Beogradu Institut za multidisciplinarna istrazivanja
Miloljub Dragoljub Luković
Univerzitet u Beogradu Institut za multidisciplinarna istrazivanja

Research Article

Keywords: Mn-Zn, Ni-Zn, Powder preparation, sintering, structural, morphological characterization

Posted Date: October 25th, 2021

DOI: https://doi.org/10.21203/rs.3.rs-968567/v1

Magnetic properties of Mn-Zn ferrites under DC bias conditions

Č. Žlebič[1], M. Milutinov[1], M. V. Nikolić[2], M. D. Luković[2]

[1]Department of Power, Electronics and Communication Engineering, Faculty of Technical Sciences, University of Novi Sad, Dositeja Obradovica 6, Novi Sad, Serbia

[2]Institute for Multidisciplinary Research, University of Belgrade, Kneza Viseslava 1, Belgrade, Serbia

Abstract

The influence of milling time and sintering temperature on the DC bias characteristics of Mn-Zn ferrite samples were analyzed in this work. Mn-Zn ferrite powder with the chemical composition of $Mn_{0.63}Zn_{0.37}Fe_2O_4$ - 93 wt % and Fe_2O_3 - 7 wt % was used. Powders was additionally milled in a planetary ball mill for 1h, 2h and 4h. Green toroid shaped samples made from each of the four powders were sintered for 2 hours at maximum temperatures of 1050 ºC, 1100 ºC, 1200 ºC, and 1300 ºC. Each sample were tested under the applied DC magnetic field in the range of 0 to 500 A/m. The best DC bias characteristics under the influence of the external H_{DC} field, was shown by samples sintered at 1050 °C and 1200 °C. With regard of milling time, the best DC bias characteristics are obtained for the starting powder samples, (ie. 0h milling time) and for the samples that are milled for 2h.

1 Introduction

The chemical composition, technological process, and sintering temperature determine the electric and magnetic properties of Mn-Zn and Ni-Zn ferrite materials making them suitable for a particular application in electrical engineering. The technological process of making ferrite materials consists of the preparation of ferrite powder, its pressing and finally sintering.

Due to the widespread use of ferrite inductors, the tunability of these components under the influence of DC current is very important as it allows setting the optimal performance of electronic circuits. Many dopants have been added into Mn-Zn and Ni-Zn ferrites, such as SnO_2, Nb_2O_5, $CaCO_3$, Co_2O_3, Bi_2O_3, SiO_2, to obtain improved frequency stability and increased initial permeability and better DC bias characteristics [1-10].

In this paper, the effects of milling and sintering temperature on the DC bias characteristics of Mn-Zn ferrite samples have been investigated. Changing the length of grinding time and values of sintering temperatures affect the structural characteristics that determine the magnetic properties of the ferrite material. Our goal is to determine the ratio of the grinding time and the value of sintering temperature in order to get the sample with the best DC bias characteristics. Grinding time and sintering temperature are effective ways of controlling the grain size of the initial powder and thus obtaining a material with desired magnetic properties [11]. However, one should be careful that grinding does not take long in order to prevent significant powder agglomeration. The

sintering temperature should also be taken into account as insufficiently high and too high temperatures may degrade the magnetic properties of ferrite samples [12].

2 Experimental procedure

2.1 Powder preparation, sintering, structural and morphological characterization

Commercial Mn-Zn ferrite powder with the chemical composition $Mn_{0.63}Zn_{0.37}Fe_2O_4$ - 93 wt % and Fe_2O_3 - 7 wt % was used. The code name of this starting powder is M-30. It was additionally milled in a planetary ball mill for 60, 120 and 240 minutes. Detailed characterization of the starting and milled powders by XRD and SEM was previously performed and given by Milutinov et al [13] and Labus et al [14]. Green toroid shaped samples (6 mm outer and 3 mm inner diameter, 2 mm high) made from each of the four powders were sintered for 2 hours at maximum temperatures of 1050 ^oC, 1100 ^oC, 1200 ^oC, and 1300 ^oC. Applying this technique, a total of 16 toroidal shaped samples were fabricated. The samples are denoted as S-A-B, where A presents the sintered temperature and B is the milling time in hours. For example, S-1100-2 is a sample sintered at 1100 ^oC and made from powder milled 2 hours (120 minutes). Scanning Electron Microscopy (SEM) micrographs of freshly cleaved toroid sintered samples were recorded on a TESCAN Electron microscope VEGA TS 5130MM device.

2.2 Characterization of magnetic properties

Measurements of the change in permeability of the samples under different DC-bias magnetic fields were performed using an HP4194A impedance analyzer with a 41941A impedance probe kit and DC-bias current source Voltcraft 2403 PRO. The measurements were performed in a frequency range from 250 kHz to 100 MHz. Applying Ampere's law, the DC magnetic field inside the core was calculated as

$$H_{DC} = \frac{N \cdot I_{DC}}{l_e}, \tag{1}$$

where $N = 14$ represent wire turns, I_{DC} is the DC-bias superposition current (range 0-500 mA) and $l_e = 14$ mm is the effective core length. Due to the ratio between the number of turns to the core's effective length of 1000, the applied DC magnetic field is in the range of 0 to 500 A/m.

3 Results and discussions

3.1 Microstructures of tested samples

Previous detailed XRD and SEM investigation of the starting powder (M-30) and milled powders (60, 120 and 240 minutes) showed that it consisted of a mixture of $Mn_{0.63}Zn_{0.37}Fe_2O_4$ and hematite (Fe_2O_3) with irregularly shaped particles [13, 14]. Milling of the powder leads to a reduction of grain size and broadening of XRD peaks. The crystallite size reduced with an increase

in milling time from 39.4 nm (0 min) to 13.7 nm (240 min) for $Mn_{0.63}Zn_{0.37}Fe_2O_4$ and 46.9 nm (0 min) to 18.1 nm (240 min) for α-Fe_2O_3 [13] as shown in Fig. 1.

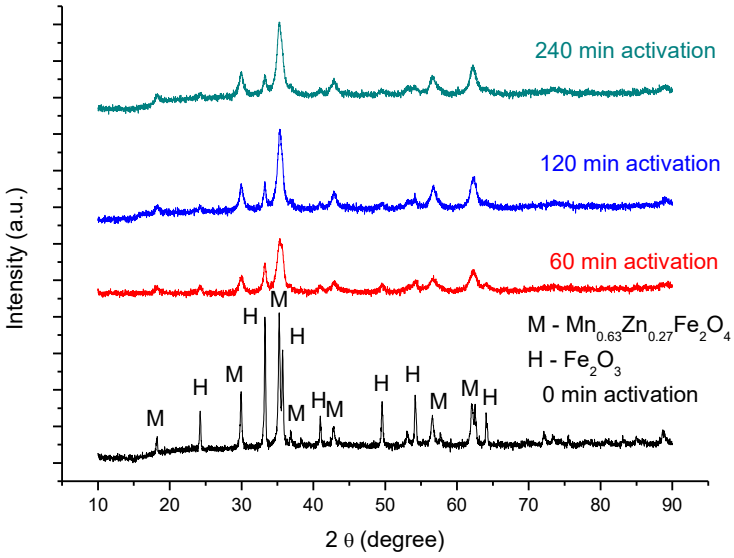

Fig. 1. XRD patterns measured for starting (M-30) and milled (60, 120 and 240 min) powders

As described in detail in our previous paper [13], the increase in sintering temperature leads to an increase in sample density more rapidly for lower sintering temperatures (800-1100°C) and more slowly at higher sintering temperatures (1100-1300°C). The milling process leads to slightly higher overall density values, compared to the density determined for samples obtained by sintering the starting non-milled powder, as shown in Table 1. However, longer milling time leads to only very slightly higher density values.

Table 1 Average density (in g/cm^3) and percentage of theoretical density (ρ_T = 5.1 g/cm^3) determined for toroid samples sintered in the temperature interval 1050 – 1300°C

Sample sintering temperature (°C)	Milling time of starting powder (minutes)			
	0	60	120	240
1050	4.48 (87.8 %)	4.72 (90.6 %)	4.70 (92.2 %)	4.71 (92.3 %)
1100	4.74 (93.0 %)	4.89 (94.7 %)	4.88 (95.7 %)	4.89 (95.9 %)
1200	4.83 (94.8 %)	4.96 (96.5 %)	4.95 (97.0 %)	4.96 (97.2 %)
1300	4.86 (95.3 %)	4.98 (97.0 %)	4.98 (97.6 %)	4.99 (98.0 %)

SEM images of freshly cleaved sintered toroid samples show that both the sintering temperature and milling time of the starting powder have an influence on the resulting sample microstructure as shown in Figs. 2 and 3. These figures show the ranges of grain size for all prepared samples, as well.

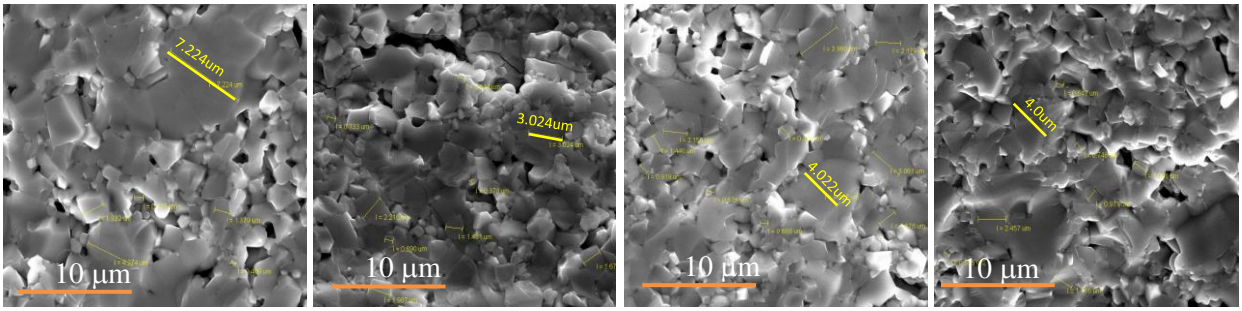

S-1050-0
Grain size 0.4 – 7.2 µm

S-1050-1
Grain size 0.38 –3.0µm

S-1050-2
Grain size 0.40 –4.0µm

S-1050-4
Grain size 0.55 –4.0µm

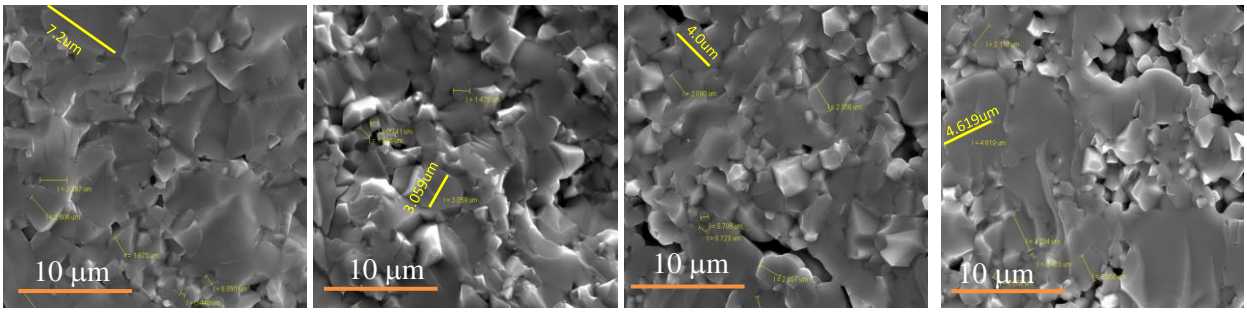

S-1100-0
Grain size 0.44 –7.2µm

S-1100-1
Grain size 0.74 –3.1µm

S-1100-2
Grain size 0.71 –4.0µm

S-1100-4
Grain size 0.66 –4.6µm

Fig. 2. SEM micrograph of Mn-Zn samples sintered at 1050°C and 1100°C using the starting powder (0) and the powders milled for 60 (1), 120 (2), and 240(4) min.

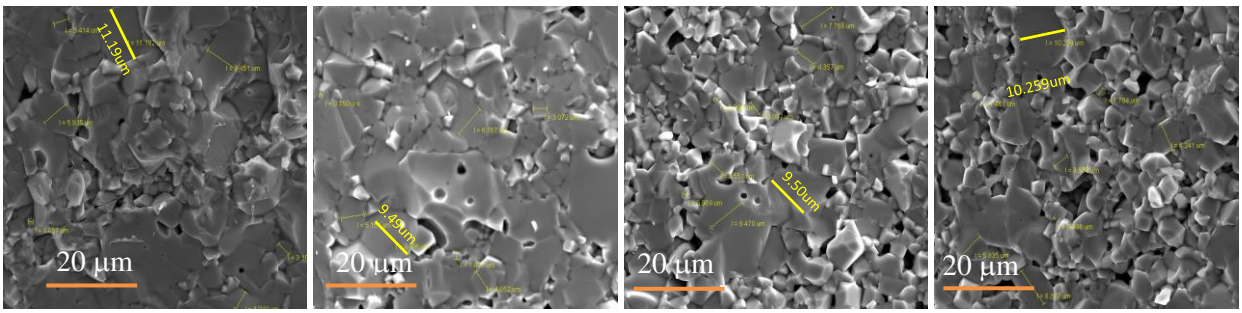

S-1200-0
Grain size 1.0 –11.2µm

S-1200-1
Grain size 0.75 –9.5µm

S-1200-2
Grain size 0.86– 9.5µm

S-1200-4
Grain size 0.5 –10.3µm

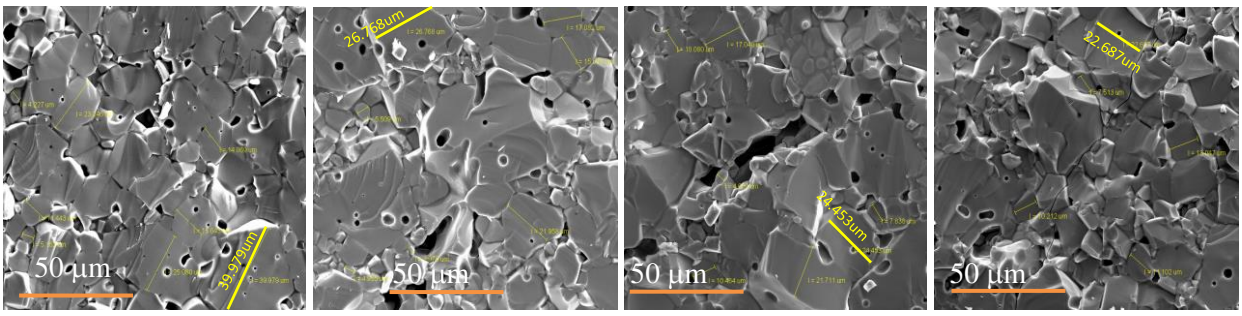

S-1300-0	S-1300-1	S-1300-2	S-1300-4
Grain size 3.0 – 40 µm	Grain size 2.9 –26.8µm	Grain size 4.0 –24.5µm	Grain size 4.0 –22.7µm

Fig. 3. SEM micrograph of Mn-Zn samples sintered at 1200 °C and 1300 °C using the starting powder (0) and the powders milled for 60 (1), 120 (2), and 240(4) min.

By observing the influence of the sintering temperature, it could be found that at 1050 °C (Fig. 2), the sample density is the lowest (between 87.8 and 92.3 %). An inhomogeneous microstructure was obtained consisting of larger sintered agglomerates, smaller grains, and noticeable open porosity. At this sintering temperature, the influence of additional milling is reflected in a reduction of overall grain size (60 minutes of milling), though prolonged milling does not further noticeably reduce the grain size and the sample density is only slightly higher and almost the same for 120 and 240 minutes of starting powder milling.

Sintering at 1100 °C leads to a denser (93-95.9%) more homogenous microstructure, though some small grains remain (Fig. 2). Milling reduced grain size (60 minutes), but larger pores/cracks start to appear for longer milling times (120 and 240 minutes).

Sintering at 1200 °C results in grain growth, where the grain size is almost double that at 1100 ºC. Besides open pores, between larger sintered grains/agglomerates, closed pores can be noticed (Fig. 3). Milling of the starting powder leads to slightly smaller grains and greater participation of smaller grains, and large crack-like pores, especially for longer milling times of 120 and 240 minutes. A noticeably inhomogeneous microstructure was obtained when the starting powder was milled for 240 minutes, where we can note large grains/agglomerates surrounded by smaller grains and large crack-like pores. The sample density is slightly higher and increases slightly as milling time increases.

Sintering at 1300 °C leads to further grain growth, with grains about 5 times larger than at 1100 °C. Open and closed pores are noticeable. Milling of the starting powder leads to a more inhomogeneous structure, especially noticeable for longer milling times (120 and 240 minutes). The sample density is also slightly higher and increases slightly with the milling time (Fig. 3).

3.2 Influence of DC-bias magnetic field

Figure 4 shows the frequency characteristics of four fabricated samples sintered at four different temperatures made of the powder which was milled for 1 hour. The cut-off frequency of all observed samples is about 10 MHz. On the diagram on the left side, only the AC magnetic field is applied, while on the diagram on the right a DC magnetic field of 500 A/m is applied. The sample S-1050-1 has the lowest permeability and the highest cut-off frequency. The applied DC magnetic field does not have a significant influence on the cut-off frequency for this sample. The permeability of S-1100-1 is reduced by a factor of 1.7 (40%) but the cut-off frequency is shifted from 10 MHz up to about 30 MHz. The applied DC field did not change the cut-off frequency for the sample S-1200-1. The permeability of the sample S-1300-1 became more stable below 10 MHz, after a DC magnetic field was applied.

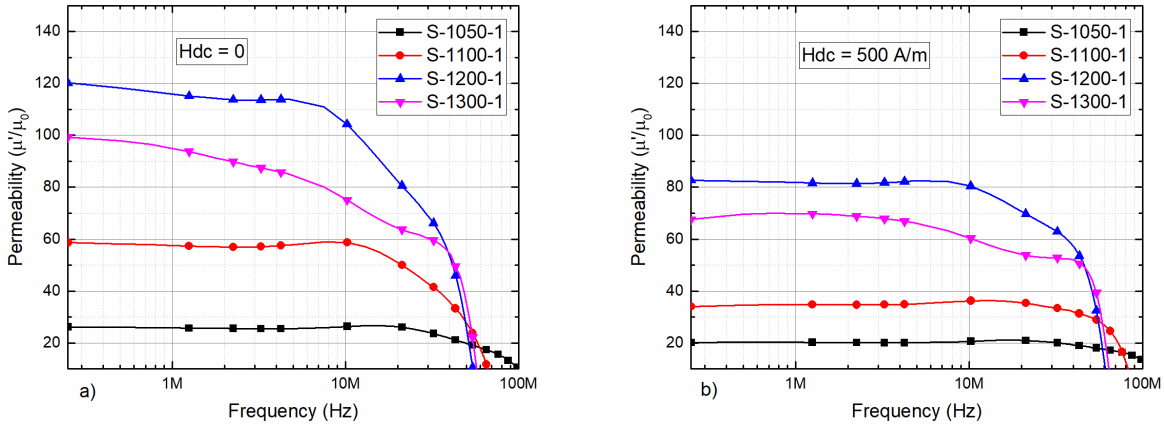

Fig. 4. The real part of the magnetic permeability of samples made of powder milled for 1 hour, without applied DC magnetic field (a) and with 500 A/m DC magnetic field.

Figure 4 shows the influence of only one value of the DC field on samples made from only one prepared powder. Further analysis focuses on presenting the influence of the DC field in more detail, by observing the samples made from the starting powder and milled powders, as well.

Figure 5 shows the real part of the sample permeability at 1 MHz for four milling times (0 h, 1 h, 2 h, 4 h), as a function of the DC magnetic field H_{DC}. The time of 0 h stands for starting powder, which is not milled. From Fig. 4a, we can see that for samples made of the starting powder, the real part of the permeability increases with increasing the sintering temperature. The lowest relative permeability was obtained for S-1050-0 while the highest was obtained for S-1300-0. Without a DC magnetic field, it is 25 for S-1050-0, and it rises to 90 for S-1300-0, increasing by more than 3 times. Applying the milling process, the permeability increases but it depends on the sintering temperature. The differences in initial permeability values are due to the increase in grain size as a result of an increase in sintering temperature. Samples made of milled powder and sintered at 1200 °C and 1300 °C which have nearly the same permeability, have much higher permeability

compared with the samples sintered at 1050 °C and 1100 °C. If the starting powder is milled for 1 hour, the samples exhibit the highest permeability, regardless of the sintering temperature. This leads to the conclusion that further milling will not bring about any improvement.

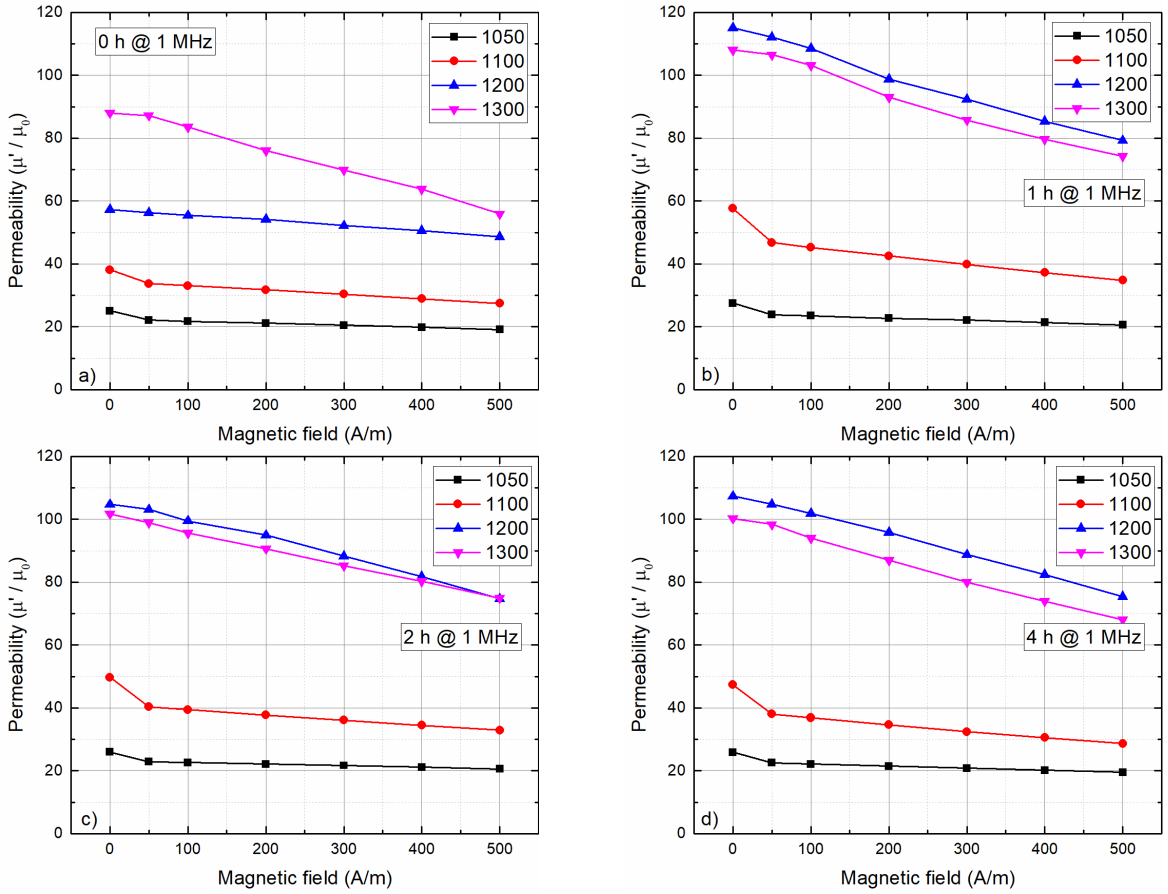

Fig. 5. The real part of magnetic permeability versus DC-bias magnetic field HDC at the frequency of 1 MHz with sintering temperature as a parameter, for samples made of starting powder (a), and powder milled for 1 hour (b), 2 hours (c) and 4 hours (d).

The applied DC magnetic field has a different influence on the permeability of analyzed samples. The DC magnetic field has increased from 0 to 500 A/m. As figure 5 shows, samples S-1050- and S-1100-, with initial lower permeability, experience a slower decrease of permeability, compared with samples S-1200 and S-1300. For samples sintered at 1050 °C and 1100 °C, the permeability tendency change is similar, regardless whether they are made of the starting or milled powder (Fig. 4). For samples sintered at 1200 °C and 1300 °C, the permeability decreases faster if a milled powder is used.

With $H_{DC25\%}$ we have denoted the value of DC-bias magnetic field for which the permeability of tested ferrite samples is reduced by 25% from the initial value. Higher values of $H_{DC25\%}$, lead to better DC-bias characteristics of ferrite samples. We have defined $H_{DC25\%}$ instead of $H_{50\%}$ or $H_{70\%}$ as in [6], [7], [8] for NiCuZn ferrites because we want to use these cores in engineering applications where smaller DC-bias ranges are preferred. Table 2 shows the values of $H_{DC25\%}$ of tested ferrite cores as a function of milling time and sintered temperature.

Table 2 HDC25% of fabricated samples as a function of milling time and sintered temperature

	0 h	1h	2h	4h
1050 °C	500 A/m	> 500 A/m	> 500 A/m	> 500 A/m
1100 °C	426 A/m	173 A/m	246 A/m	171 A/m
1200 °C	> 500 A/m	389 A/m	449 A/m	427 A/m
1300 °C	363 A/m	371 A/m	472 A/m	383 A/m

The permeability spectrum of Mn-Zn ferrite can be decomposed into two magnetization mechanisms; spin rotation and domain wall motion [15], [16]. The permeability of Mn-Zn ferrites at low frequencies is attributed to the movement of domain walls [15]. It has been reported that the critical size of a single-domain state in Mn-Zn ferrites is 3-4 μm, but with the analytical 2/3 μ correction, the calculated transitions are in the 0.2-5 μm range [17]. Examining the range of grain sizes in Fig. 2 and Fig. 3, we can conclude that the grains of samples sintered at 1050 °C and 1100 °C can be considered in the mono-domain state. The domain structure in grains for samples sintered at 1200 °C and 1300 °C transfers from a single-domain to a multiple-domain state. As the H_{DC} field increases, the sample domain walls gradually disappear and become negligible in the magnetization process.

The best DC bias characteristics were measured for the samples sintered at 1050 °C, which has the smallest component of domain wall motion, and in addition has the lowest sample density. For samples made using the starting powder, the value of $H_{DC25\%}$ is 500 A/m. With increasing milling time, $H_{DC25\%}$ rises and exceeds 500 A/m.

The samples sintered at 1100 °C show the best results of $H_{DC25\%}$ for the starting powder and the value of $H_{DC25\%}$ is 426 A/m. With increasing milling time, values of $H_{DC25\%}$ decreased.

For samples sintered at 1200 °C, the highest value of $H_{DC25\%}$ is measured for the sample made from the starting powder and it exceeds 500 A/m. By milling it, the value of the $H_{DC25\%}$ field decreases, but it does not go below 389 A/m.

Concerning samples sintered at 1300 °C, the value of the $H_{DC25\%}$ field increases with increasing milling time and the highest value of the $H_{DC25\%}$ field has for the milling time of 2 hours ($H_{DC25\%}$ = 472 A/m).

4 Conclusion

This paper presents Mn-Zn ferrites prepared using a starting and additionally milled powder, sintered at four different temperatures (1050 °C, 1100 °C, 1200 °C and 1300 °C). Examining the DC-bias characteristics for H_{DC} field values up to 500 A/m in the frequency range up to 100 MHz and in more detail at the frequency of 1MHz, we came to the following conclusions:

- The permeability depends on the powder used, the sintering temperature, and the DC-bias. As the permeability without the DC-bias increases, the influence of the DC-bias on the permeability grows.
- The DC-bias reduces permeability regardless of the manufacturing process.

- The DC-bias increases the cut-off frequency for samples sintered at 1050 °C and 1100 °C.

At the frequency of 1 MHz it could be concluded that:

- The best DC-bias characteristics, ie. the smallest change in the real part of permeability under the influence of the external H_{DC} field, was shown by samples sintered at 1050 °C. These samples have an $H_{DC25\%}$ field value of 500 A/m and above, regardless of milling times.
- The next best DC-bias characteristics were determined in cores sintered at 1200 °C, which have the $H_{DC25\%}$ field value higher than 389 A/m, regardless of milling times.
- If it is necessary to choose the optimum milling time for which at all sintering temperatures samples have the best DC-bias characteristics, this would be a time of 0 h, ie. starting powder samples and 2h. The values of all $H_{DC25\%}$ field are higher than 246 A/m.

5 Acknowledgment

This work has been performed as part of projects III45014 and TR32016 financed by the Ministry for Education, Science and Technological Development of the Republic of Serbia.

6 References

[1] G. Wu, Z. Yu, K. Sun, R. Guo, B. Wang, X. Jiang, L. Li, Z. Lan, Excellent Tunable DC Bias Superposition Characteristics for Manganese Manganese-Zinc Ferrites, IEEE Trans. Power Electron. (2019) 1-1. https://doi.org/10.1109/TPEL.2019.2921868.

[2] K. Jiang, K. Li, C. Peng, Y. Zhu, Effect of multi-additives on the microstructure and magnetic properties of high permeability Mn-Zn ferrite, J. Alloy Compd. 541 (2012) 472-476. https://doi.org/10.1016/j.jallcom.2012.06.113.

[3] Y. Liu, S. He, Development of high DC-bias Mn–Zn ferrite working at frequency higher than 3MHz, J. Alloy Compd. 489 (2010) 523-529. https://doi.org/10.1016/j.jallcom.2009.09.099.

[4] H. Shokrollahi, K. Janghorban, Influence of additives on the magnetic properties, microstructure and densification of Mn–Zn soft ferrites, Mater. Sci. Eng. B. 141 (2007) 91-107. https://doi.org/10.1016/j.mseb.2007.06.005.

[5] V.T. Zaspalis, V. Tsakaloudi, M. Kolenbrander, The effect of dopants on the incremental permeability of MnZn-ferrites, J. Magn. Magn. Mater. 313 (2007) 29-36. https://doi.org/10.1016/j.jmmm.2006.11.210.

[6] L. Huan, X. Tang, H. Su, H. Zhang, Y. Jing, B. Liu, Effects of SnO_2 on DC-Bias-Superposition Characteristic of the Low-Temperature-Fired NiCuZn Ferrites, IEEE Trans. Magn. 50 (2014) art. no. 2006104. https://doi.org/10.1109/TMAG.2014.2324553.

[7] A. Wang, H. Su, X. Tang, Y. Li, Z. Xu, Y. Jing, Comparison between Nb_2O_5 and $CaCO_3$ additions on the DC-bias superposition characteristic of low-temperature-fired NiCuZn ferrites, J. Mater. Sci.: Mater. Electron. 29 (2018) 14605-14611. https://doi.org/10.1007/s10854-018-9596-9

[8] S. Yan, L. Dong, Z. Chen, X. Wang, Z. Feng, The effect of the microstructure on the DC-bias superposition characteristic of NiCuZn ferrite, J. Magn. Magn. Mater. 353 (2014) 47-50. https://doi.org/10.1016/j.jmmm.2013.10.006.

[9] C. Ouyang, S. Xiao, J. Zhu, W. Shi, Microwave sintering versus conventional sintering of NiCuZn ferrites. Part II: Microstructure and DC-bias superposition characteristics, J. Magn. Magn. Mater. 407 (2016) 182-187. https://doi.org/10.1016/j.jmmm.2016.01.081.

[10] C. Sujatha, K. Reddy, K. Babu, A. Reddy, M. Suresh, K. H. Rao, Effect of Mg substitution on electromagnetic properties of NiCuZn ferrite, J. Magn. Magn. Mater. 340 (2013) 38-45. https://doi.org/10.1016/j.jmmm.2013.03.027.

[11] Y. Matsuo, K. Ono, T. Hashimoto, F. Nakao, Magnetic Properties and Mechanical Strength of MnZn Ferrite, IEEE Trans. Magn. 37 (2001) 2369-2372. https://doi.org/10.1109/20.951175.

[12] E. M. M. Ibrahim, The effect of sintering time and temperature on the electrical properties of MnZn ferrites, Appl. Phys. A. 89 (2007) 203-208. https://doi.org/10.1007/s00339-007-4088-4.

[13] M. Milutinov, M. V. Nikolic, M. D. Lukovic, N. Blaz, N. J. Labus, Lj. Zivanov, O. S. Aleksic, Influence of starting powder milling on structural properties, complex impedance, electrical conductivity and permeability of Mn-Zn ferrite, J. Materi. Sci.: Mater. Electron. 27 (2016) 11856-11865. https://doi.org/10.1007/s10854-016-5328-1

[14] N. J. Labus, Z. Z. Vasiljevic, O. S. Aleksic, M. D. Lukovic, S. Markovic, V. B. Pavlovic, S. Mentus, M. V. Nikolic, Characterization of $Mn_{0.63}Zn_{0.37}Fe_2O_4$ Powders After Intensive Milling and Subsequent Thermal Treatment, Sci. Sintering 49 (2017) 455-467. doi: https://doi.org/10.2298/SOS1704455L

[15] T. Tsutaoka, T. Kasagi, K. Hatakeyama, Magnetic Field Effect on the Complex Permeability for a Mn-Zn Ferrite and its Composite Materials, J. Eur. Ceram. Soc. 19 (1999) 1531-1535. https://doi.org/10.1016/S0955-2219(98)00474-9

[16] H. Su, H. Zhang, X. Tang, Y. Jing, Z. Zhong, Complex permeability and permittivity spectra of polycrystalline Ni–Zn ferrite samples with different microstructures, J. Alloys Compd. 481 (2009) 841-844. https://doi.org/10.1016/j.jallcom.2009.03.133

[17] P.J. van der Zaag, New views on the dissipation in soft magnetic ferrites, J. Magn. Magn. Mater. 196-197 (1999) 315-319. https://doi.org/10.1016/S0304-8853(98)00732-X